

# Three-dimensional reconstruction of *Monochamus alternatus* galleries using CT scans

**Huawei Yang**

Shandong Agricultural University

**Jianfeng Qiu** (✉ [jfqu100@163.com](mailto:jfqu100@163.com))

Shandong First Medical University

**Shangkun Gao**

Shandong Agricultural University

**Jinxing Wang**

Shandong Agricultural University

**Wen Li**

Shandong First Medical University

---

## Article

### Keywords:

**Posted Date:** April 13th, 2022

**DOI:** <https://doi.org/10.21203/rs.3.rs-1513333/v1>

**License:**   This work is licensed under a Creative Commons Attribution 4.0 International License.

[Read Full License](#)

---

# Abstract

Cerambycid pests are wood-boring, cryptic and extremely difficult to control – features that have made them a global problem. In this study, we present a method of scanning the galleries of *Monochamus alternatus* using CT technology to obtain their systematic structure via three-dimensional (3D) reconstruction, so as to clarify the gallery types and their structural parameters. We performed TLC scanning on wood segments damaged by *M. alternatus* using a 128-row spiral CT GE Revolution EVO to obtain 64-layer CT scanned images. From the scanned images, we were able to clearly identify the beetle larvae and their galleries. The galleries were clearly delineated from the peripheral xylem, except parts that were blocked by frass-feces mixture, which were slightly blurred. Three-dimensional reconstruction of the galleries showed that most of the gallery types were C-shaped, and a few were S-shaped or Y-shaped. There was only one larva per gallery, and galleries were separate. The vicinity of the entrance hole and the anterior part of the pupal chamber were blocked with frass-feces mixture. There were no significant differences among the galleries' parameters, such as the width of the entrance holes, tunneling depth, vertical length, blockage length and volume, total length of the galleries and boring volume. With MIMICS image processing software, the images of each layer were made into a composite image, providing an effective way to visualize the 3D distribution of galleries. Using the methodology outlined in this study, both a single gallery structure and the spatial distribution of multiple galleries of *M. alternatus* can be shown, and the specific parameters of galleries can also be accurately calculated, which provides new ideas and methods for carrying out ecological and scientific research and precise prevention and control techniques of *M. alternatus*.

# Introduction

Longhorn beetles (Cerambycidae) are an important group of wood-boring species within the Coleoptera (Jiang et al., 1989; Aukema et al., 2011). In China, species such as *Monochamus alternatus*, *Anoplophora glabripennis*, *A. chinensis*, *Apriona swainsoni*, *Batocera horsfieldi*, *Massicus raddei* and *Aromia bungii* cause extensive tree damage, resulting in considerable economic losses and serious threats to ecological security (Anbutsu et al., 1997; Wang, 1998; Liu et al., 1999; Nowak et al., 2001; Yang et al., 2010; Tang et al., 2011; Wang et al., 2015). These longicorn beetles share the common features of cryptic habits, long and irregular generations, high fecundity, and rapid and stable population proliferations. These species are also highly adaptable, have diverse hosts (and therefore good food resources), as well as high environmental tolerance and survival rates. Moreover, they have few natural enemies and weak natural control. Despite their weak dispersal ability, human activities enable them to spread easily over long distances. The beetles' activity eventually leads to the hollowing of host plant branches, weakening of host trees, or even death of the entire plant or of whole forest areas (Wei et al., 2007; Lv et al., 2015; Kundanati et al., 2020). The lack of research on the biological characteristics during the hidden life stage of wood-boring insects poses difficulty in species identification, quarantine and control.

Dissecting heavily infested wood is the most direct and traditional solution, but this method destroys the integrity of the wood, and is time-consuming and laborious. At present, nondestructive detection methods

for wood-boring pests in the hidden life stage mainly include manual detection, sound detection and other methods. Manual detection methods rely on the biological reactions of winged insects to physical and chemical substances, such as trap lamps and commercial insect pheromones and attractants. These methods are not only time and labor-intensive, but also fail to attract wood-boring pests living inside trees, and are greatly affected by weather (Su et al., 2008). The sound detection method can be used for early detection of wood-boring pests without harming trees. Through characteristic sound signals, the species of pests can be identified and the number of individuals estimated, so as to carry out targeted prevention and control, which greatly reduces the cost of pest detection. However, this method is limited by the activity state of borers and the sensitivity of sound signal acquisition and analysis equipment. Meanwhile, it is necessary to determine the specific physical parameters of various insects' sounds and establish a database (Bilski et al., 2017; Gorres et al., 2019; Sun et al., 2020). In addition, X-ray detection based on X-ray autoradiography can also act as an auxiliary tool for longicorn beetle quarantine in wood import and export. Through this method, longicorn beetle larvae and the amount of wood damage can be directly observed; however, equipment is too heavy to be used in the field, and X-rays pose a risk of harm to humans (Cruvinel et al., 2003).

*Monochamus alternatus* (Coleoptera: Cerambycidae) is the most destructive wood-boring pest in East Asia (Hu et al., 1997). It is mainly harmful to *Pinus massoniana*, *P. elliotii*, *P. taeda* and *P. thunbergii*, *Cedrus deodara*, *Larix gmelinii*, *Abies fabri*, *Picea asperata* and *Malus pumila* (Yang, 2002). This species directly kills the host tree via wood drilling by larvae, or indirectly kills the host plants via pine wood nematode disease transmitted by adults during feeding, which poses a major threat to forestry production and ecological security (Mamiya et al., 1972). Figuring out the boring characteristics of longhorn beetles in the larval stage is important for the study of their survival and reproduction. Discovering the weak link in the larval stage is key to reducing the population of adults, and can effectively prevent and control pine wood nematode disease. Zhao (2005) reported in detail the biological and ecological characteristics of *M. alternatus* larvae in the gallery stage, and the results showed that the gallery distribution was closely related to tree height, diameter at breast height, plant height and trunk bark thickness. Trees with a bark thickness of 1.1–2.0 mm and 3.1–4.0 mm had the largest gallery distribution in *P. massoniana* and *P. taiwanensis*, respectively. To prevent congeners from entering the tunnel, the larva made a warning sound, which lasted for a mean of 2 min 35 s. Togashi et al. (2008) artificially inoculated *M. alternatus* larvae into the wood segments of different pine species, and the results showed that *M. alternatus* larvae of the same weight could construct deeper and longer pupal chambers in the soft xylem of the tree. Gao et al. (2022) obtained the species' gallery structure parameters by dissecting heavily infested wood, and the results showed that *M. alternatus* larvae had a single gallery structure, mostly C-shaped, unconnected with each other, and blocked to varying degrees by a frass-feces mixture near the entrance holes. Gallery length was unrelated to host plant species and larvae size. However, this method is based on dissecting a large amount of damaged wood, making it labor-intensive, and the manual measurement index data is imprecise.

Internal structure models established by X-ray computer tomography (CT) and three-dimensional (3D) image reconstruction have enabled great achievements in medicine and industry (Wang et al., 2019), and

have advanced the methods for the spatial localization of wood-boring beetles and the evaluation of the degree of damage in tree trunks (Cruvinel et al., 2003; Ma et al., 2012; Lyons et al., 2020). The 128-row spiral CT GE Revolution EVO has been greatly improved in terms of temporal and spatial resolution, providing the necessary technical support for 3D reconstruction of longhorn beetle galleries. This study aims to achieve the following objectives with this technique: 1) determine the number and distribution of *M. alternatus* galleries in the host wood segment, and whether the characteristics of insects, frass and boring in a single gallery can be clearly distinguished by CT scanning; 2) use 3D reconstruction technology to accurately calculate *M. alternatus* gallery structural parameters, including gallery volume, frass blockage volume, tunneling depth and inner diameter of entrance hole; 3) provide technical support using these methods for prevention and control strategies of *M. alternatus* in the hidden wood-boring stage.

## Methods

### 1.1 Scanning wood segments

The scanned wood segments (length 100cm×diameter 17.5cm) were taken from *Pinus densiflora* damaged by *M. alternatus* in the Sorai Mountain view area, in Tai'an city, Shandong Province. Some *M. alternatus* in the xylem of the wood segments were still in the larval stage and their galleries were incomplete. Some had emerged, and their galleries were complete; however, some of the galleries at the ends of the segments were incomplete, i.e., where the segments had been removed from the host tree.

### 1.2 Equipment and software

The 3D reconstruction software used in this study was Materialise Mimics Medical 21.0 (Materialise, Belgium, provided by the School of Radiology, Shandong First Medical University, authorized). We used Adobe Photoshop CC (2019) for image annotation, and MS Office 2016 for text editing and generating charts. We conducted CT scans on a 128-slice spiral CT GE Revolution EVO (provided by the CT Laboratory at the School of Radiology, Shandong First Medical University).

### 1.3 Data collection

The scanning parameters were as follows: detector width (mm): 40.0, pitch (mm): 0.516, speed (mm/rotation): 120.62, layer thickness (mm): 0.625, rotation time (s): 1.0. Multiple CT images were obtained by scanning different wood segments.

### 1.4 Three-dimensional reconstruction of *M. alternatus* galleries

Three-dimensional reconstruction of gallery scan images was performed using MIMICS (2019) software. Some galleries were blocked by the frass-feces mixture deposited by the *M. alternatus* larvae during feeding, which made it difficult to distinguish the galleries from the xylem in CT images. Therefore, galleries were actively selected to be reconstructed. First, we created a new mask and selected the threshold interval as 0. Then we used the Edit Mask function in the Segment window to manually select

*M. alternatus* galleries in each tomographic image. Then we used the Region Grow function of MIMICS to select galleries more accurately to obtain the gallery images after 3D reconstruction. After the above steps, the gallery structure was continuous but not smooth. The Smoothing function of 3D Objects was used to optimize the reconstructed gallery to achieve a more realistic display effect. The trunk and the internal gallery system were reconstructed to show the spatial distribution of multiple galleries in the trunk. We used the Split Mask function to separate each gallery from the overall reconstruction portion, allowing each gallery to be viewed individually.

### 1.5 Determination of gallery parameters

Maximum width of the entrance hole: first, we found the widest part of the entrance hole and made a straight line, which was nearly parallel to the gallery, along the entrance hole. Then we made a second straight line at a 90-degree angle to the first line to connect the widest part of the entrance hole. The length of the line segment was the maximum width of the entrance hole. The total length of the gallery was the length from the center of the entrance hole to the center of the emergence hole. For the reconstructed gallery, we used the Spline function in the Analyze window to draw a curve along the center part of the gallery, then we obtained the center line of the gallery and its length data. The length of the line was approximately the length of the gallery.

Reconstruction of blocked galleries and their lengths: blocked galleries were consistent with the reconstruction of the other galleries and the measurement of the total length of the gallery, respectively.

Boring depth: we sought the largest plane of the gallery entrance hole and intrusion depth. Taking the annual ring of the wood as the center and the distance between the annual ring and the entrance hole as the radius, we drew a circle, requiring the circle to pass the entrance hole and the arc of the circle to coincide with the wood edge as much as possible. The diameter of the deepest intrusion point was made with the center of the circle as the starting point, and then taking the deepest intrusion point as the starting point, a line segment with the same end point was made along this diameter. The length of this line segment was the maximum intrusion length.

Complete gallery volume and blocked gallery volume: volume data could be directly viewed and calculated after the reconstruction was completed.

## Results

### 2.1 Scanning images of *M. alternatus* galleries

The format used for scanning data of the wood segments was DICOM. We opened the data files with MIMICS, and the CT images showed that the color of the galleries was significantly darker than that of the xylem, and the boundaries, boring direction, vertical and horizontal distribution of galleries were all clear. The galleries blocked by frass-feces mixture resemble xylem and were not well-distinguished. The

*M. alternatus* larvae in the galleries were white in the scanning image, but were conspicuous in the dark galleries, and their sizes were also clearly visible, as shown in Fig. 1.

## 2.2 Three-dimensional reconstruction of galleries

Using the CT scanning images, the galleries in wood segments were selected, reconstructed and saved, then the reconstruction data of corresponding galleries were obtained. The reconstruction models and data of 43 complete galleries were obtained by reconstructing five complete galleries in *P. densiflora*. When displaying the MIMICS models in the FreeForm Modeling System, the model could be zoomed in, zoomed out, rotated and comprehensively observed, as shown in Fig. 2.

H, I, J and K show views of the galleries in an entire wood segment. The relative spatial position of the galleries in the wood segment were clear. The brown parts in H were the blocked parts of the galleries. L and M showed the reconstructed galleries, and the shapes and number of galleries were clear. Each reconstructed gallery image was obtained by adjusting the transparency of the whole section or hiding the wood segments.

## 2.3 Gallery types of *M. alternatus*

The reconstructed gallery images showed that each gallery was separate and most were C-shaped (83.72%), while the remaining galleries were either S-shaped (6.97%) or Y-shaped (9.3%), as shown in Fig. 3. There was only one larva in each gallery. The three kinds of galleries were curved near the entrance holes, and at the end of the galleries were the pupal chambers, which were significantly larger than the entrance holes. The entrance holes and emergence holes of C-shaped and Y-shaped galleries were at the same end, while those of S-shaped galleries were at opposite ends. The three gallery types were all blocked by frass-feces mixture near the entrance holes and in the anterior parts of the pupal chambers. It could be seen that the larvae pushed out the mixture during feeding, and it was left in the galleries after pupation.

## 2.4 Three-dimensional reconstruction of gallery blockage

It can be seen from Fig. 4 that the volume of the blocked part of each gallery was 0–40% of the total gallery volume. Most of the galleries had blocked parts, and few had no blocked parts. From the CT images and reconstructed models, it could be seen that the blocked parts of the galleries were mostly located near the entrance holes or in the middle of the galleries.

## 2.5 Structural parameters of galleries

It can be seen from Table 1 that the parameter values of S-shaped galleries were higher than those of the other galleries, but there was no significant difference between them ( $P > 0.05$ ). There was no significant difference ( $P = 0.67$ ) in the width of the entrance holes, indicating that the head capsule width and body width of the individuals were basically the same when entering the xylem. There were no significant differences in gallery depth, vertical length, blockage length, blockage volume, or total length of the

galleries ( $P > 0.05$ ), indicating that the boring habits and behaviors of the larvae in the xylem were similar. The proportion of galleries of each type (e.g., C-shaped) that were blocked ranged from 5–65%, with a mean of 24.26%. There was no significant difference among the three types of galleries ( $P = 0.66$ ), indicating that the larvae's wood consumption and living space within the xylem were relatively fixed, and were not affected by the boring direction and behaviors.

Table 1  
Parameters of *Monochamus alternatus* galleries.

Galleries type	entrance holes width /mm	gallery depth /mm	vertical length /mm	blockage length /mm	blockage volume /mm <sup>3</sup>	total length of the gallery /mm	boring volume /mm <sup>3</sup>
C	2.90 ± 0.44	29.51 ± 8.90	47.68 ± 16.78	25.73 ± 17.10	806.59 ± 777.51	79.16 ± 25.77	2988.01 ± 274.9
S	3.10 ± 0.26	36.44 ± 5.93	51.10 ± 16.48	38.29 ± 8.69	952.73 ± 296.72	108.73 ± 17.35	3669.26 ± 794.4
Y	2.81 ± 0.27	33.11 ± 10.17	42.60 ± 10.10	30.52 ± 21.84	558.21 ± 423.15	88.49 ± 29.04	2530.80 ± 705
<i>F</i>	0.40	0.99	0.24	0.76	0.27	1.85	0.42
<i>df</i>	2, 42	2, 42	2, 42	2, 39	2, 39	2, 42	2, 42
<i>P</i>	0.67	0.38	0.79	0.47	0.77	0.17	0.66

## Discussion

The study of the distribution of wood-boring pests and their gallery construction behavior is key to exploring their survival and reproductive mechanisms and population variation, as well as the associated disaster prevention and control planning (Zhao, 2005). In this study, our CT scan results showed that the *M. alternatus* galleries were single, that is, each gallery had only one individual larva, and the galleries were independent of each other. The three-dimensional reconstruction results showed that the majority of galleries were C-shaped, which was consistent with the results obtained by dissection of damaged wood (Gao et al., 2022). In addition, the results of 3D reconstruction showed that a few of the *M. alternatus* galleries were S-shaped or Y-shaped, which also reflected the intuitive nature and comprehensiveness of the three-dimensional reconstruction method. Gallery structures vary, because in the process of boring, larvae need to make a detour when meeting host plant tree knots, or change their boring direction when encountering other larvae to avoid each other. This boring behavior not only feed conveniently, it also reduces unnecessary energy consumption in the region of obstacles (Hao et al., 2005). In this study, there were no significant differences in gallery parameters such as tunneling depth and boring volume (Table 1), which may be because of the fixed energy input of larvae while boring the gallery and constructing the pupa chamber after entering the xylem. In addition, the change of boring direction may

be related to the nutrients in the regions with different xylem height or diameters (Yang, 2010). Intraspecific and interspecific aggregations have been analyzed via longhorn beetle numbers and the spatial layout of galleries in a given space (Gregoryet, 2015). In this study, the whole section of damaged wood was 70 cm long, containing nearly ten *M. alternatus* galleries, and the regional population was large. Previous studies have shown that *M. alternatus* clusters in the host tree trunk (Gao et al., 2015; Wen et al., 2018), which may indicate that longhorn beetles choose the central area to lay eggs to avoid natural enemies and human interference during laying (Yang, 2010). However, the direction of boring and the distribution of galleries were coordinated and orderly, and did not disturb each other. That meant when insect density reached a certain level, the movement of the aggregation distribution center was blocked (mainly in the form of intraspecies competition), leading longhorn beetles to expand their space more to areas with less competition (Johnson et al., 2001). Some studies have shown that longhorn beetle larvae have formed a special communication mechanism during their evolutionary history. The hardened body wall tissue makes sound when rubbed against the gallery wall, and the abdominal side plate has an organ that detects and produces sounds, and this organ senses the sound of nearby longhorn beetle larvae. Using these organs, longhorn beetle larvae locate the movements of nearby larvae by means of the mechanism of sending and receiving sounds within the dark host trunk (Tang et al., 2005). To avoid entry by individuals of the same species, the residents of the galleries use the sound warning of rodents, thus playing an important role in regulating the degree of population aggregation, so as to effectively use the space and resources of host plants (Jiang, 1989; Wang, 2005).

The galleries formed by wood-boring pests, as represented by the *M. alternatus*, have been shown to be stereoscopic. Through dissection of the damaged wood, only local conditions can be observed. In this study, CT scanning technology clearly identified the insect body and the boring conditions of *M. alternatus*, which enabled the complete structure and distribution of galleries to be reconstructed via 3D reconstruction. Continuous scanning and three-dimensional reconstruction of galleries in different life stages better reflects the beetles' biological characteristics (e.g., food consumption, boring habit, overwintering and pupation characteristics). In this study, one or two generations of *M. alternatus* occurred in one year (Wang, 1992; Anbutsu et al., 1997). Larvae in the xylem stage had a small boring volume (approximately 30 mm<sup>3</sup>), and the structure and type of galleries were relatively simple and easy to distinguish and identify through CT scanning and three-dimensional reconstruction. Therefore, the structural characteristics and spatial distribution pattern of galleries were used as identification methods for larval species. However, the generations of species such as *Apriona swainsoni*, *Batocera horsfieldi*, *Massicus raddei* and *Aromia bungii* span 2–3 years, with longer feeding times, increased food intake, larger gallery volumes and more complex structures (Liu et al., 1999; Liu et al., 2009; Yang et al., 2010; Tang et al., 2011). In addition, some longhorn beetles with more generations may also have a variety of gallery types, or irregular galleries, including galleries that connect with each other, such as seen in *Xylotrechus quadripes*, which has two generations per year and a considerable overlap in generations. Within the same trunk, the borers' ages were inconsistent, and the galleries in the trunk occurred at different times, which led to subsequent larvae entering established galleries (Chai et al., 2020). Therefore, in future studies, sample sizes should be increased, and a database established to determine

the gallery structure for each wood-boring pest species, so as to increase the identification accuracy of subsequent testing.

In the process of feeding in the galleries, the larvae move forward and push frass and feces to the rear of the galleries by the pressing action of the hardened anterior thoracic plate, dorsal and ventral step vesicles and caudal gluteal plate (Jiang, 1989; Wang, 2005). Among longhorn beetle species, larvae have different ways of treating the frass-feces mixture in the galleries. For example, the larvae of *Anoplophora glabripennis* and *Aromia bungii* bite a circular fecal hole and push the feces out of the hole after boring a section of gallery (Niu et al., 2010; Liu, 1999). In view of the similarity between the scanning image data of galleries and wood dust and frass, the boundary between the two must be carefully observed and the galleries carefully selected to distinguish the two successfully. Our results show that in C-shaped galleries, the mixture mainly blocked the main middle section (Fig. 2I), and this blockage is likely generated during the construction of the pupa chamber. However, the mixture in other parts was pushed out of the gallery, which is not completely consistent with the report by Zhao (2005) that the larva of *M. alternatus* do not push the mixture out of the host, but fill the posterior segment of the gallery. We observed many frass-feces deposits outside the entrance holes, which, according to our many years of experience in forest investigation, would have been pushed out by larvae. Therefore, we conclude that the larva push the mixture outwards while feeding before pupation, and the mixture generated during the pupal chamber construction before overwintering remains in the gallery. To ensure the stability of the population, the borers avoid predation and parasitism by natural enemies via various covert means. For example, the depth of dung beetle tunnels has been shown to be a key variable affecting the rate at which the beetles are parasitized (Arellano et al., 2016). In the interaction between longhorn beetles and their natural enemies, the depth and length of the boring larvae galleries and the blockage by the frass-feces mixture affects their interaction with natural enemies to varying degrees. In some ichneumonid species, females laid eggs directly on host larvae by puncturing branches with their long ovipositor sheaths, and the boring depth of host larvae was a key factor affecting parasitism (Taylor, 1977). *Sclerodermus* spp. is an important parasitic pest group of longhorn beetles; the adult females penetrate the bark to search within the phloem for larvae to parasitize, but cannot enter the xylem because of the blockage of the frass-feces mixture (Jiang et al., 2015). Before the pupal chamber is constructed by the mature larvae, the fibers bitten by the upper jaw are thick and the gap is relatively large, which provides an opportunity for their smaller natural enemies to successfully colonize or prey on them via the otherwise blocked galleries. The widely used parasitoids of Coleoptera effectively parasitize mature larvae or pupae of *M. alternatus* after overwintering (Zhang et al., 2014; Gao et al., 2016), probably because the newly hatched larvae (less than 1 mm in length) can penetrate the blocked galleries to complete their parasitism.

The prevention and control of wood-boring pests is an important problem faced by researchers all over the world. At present, CT scanning and 3D reconstruction technology enable the nondestructive detection and identification of such pests, and the degree of damage by pests can be assessed through image processing. However, because of the diversity of pest species and the complexity of the harm they cause to host plants, it is still necessary to expand the amount of data collection and establish a database to ensure the detection accuracy within ecological niches and among similar species. Three-dimensional

scanning of the reconstructed gallery structure provides new ideas and methods for studying the interaction between longhorn beetles and exogenous substances in xylem by simulating the gallery environment. In addition, this technology also has great application potential in pest quarantine, the use of exogenous agents, the release of natural enemies, and the research and development of related equipment for the precise control of borer pests.

## Declarations

### Data Availability

The datasets generated during and analysed during the current study are providing in the supplementary file.

### Acknowledgments

We thank Clio Reid, PhD, from Liwen Bianji (Edanz) ([www.liwenbianji.cn/](http://www.liwenbianji.cn/)) for editing the English text of a draft of this manuscript.

### Funding

This research was supported by Shandong Provincial Natural Science Foundation, grant number ZR2021MC046, the Project of Shandong Agricultural Science and Technology Fund (Forestry Science and Technology Innovation), grant number 2019LY003, National Natural Science Foundation of China, grant number 32101538.

### Author contributions statement

J.Q. and S.G. conceived the experiment. H.Y. and J.W. conducted the experiment. H.Y. and W.L. analysed the results. All authors reviewed the manuscript.

### Additional information

The authors declare no competing interests.

### Research involving plants statement

Firstly, no direct plants were used in this study; Secondly, the plant materials used in this study, i.e. wood segments, are *Pinus densiflora* killed by pine longhorn beetle *Monochamus alternatus*, which were obtained with permission from our cooperation base Sorai Mountain view area, and did not violate the relevant regulations of forestry departments in Tai'an city, Shandong Province, China.

## References

1. Aguilera, O.D., Palma-Onetto V., Flores-Prado L., Zapata V., Niemeyer H. M.. X-ray computed tomography reveals that intraspecific competition promotes soldier differentiation in a one-piece nesting termite. *J. Entomologia Experimentalis Et Applicata*, **163(1)**, 26–34 (2017).
2. Anbutsu H., Togashi K. Deterred oviposition of *Monochamus alternatus* (Coleoptera: Cerambycidae) on *Pinus densiflora* bolts from oviposition scars containing eggs or larvae. *J. Appl. Entomol. Zool.* **31**, 481–488 (1996).
3. Anbutsu H., Togashi K. Effects of spatio-temporal intervals between newly-hatched larvae on larval survival and development in *Monochamus alternatus* (Coleoptera: Cerambycidae). *J. Res Popul Ecol* **39**, 181–189 (1997).
4. Arellano L. A novel method for measuring dung removal by tunneler dung beetles (Coleoptera: Scarabaeidae: Scarabaeinae) in pastures. *J. The Coleopterists Bulletin*, **70(1)**, 185–188 (2016).
5. Aukema J. E., *et al.* Economic impacts of nonnative forest insects in the continental. *J. United States. PLoS One*, **6**, 1–7 (2011).
6. Bilski P., Bobinski P., Krajewski A., Witomski P. Detection of wood boring insects' larvae based on the acoustic signal analysis and the artificial intelligence algorithm. *J. Archives of acoustics: Journal of Polish Academy of Sciences.* **42(1)**, 61–70 (2017).
7. Cruvinel P. E., Naime J.M., Borges M., Macedo Á., Zhang A. Detection of beetle damage in forests by X-ray CT image processing. *J. Revista rvore*, **27(5)**, 1095–1100 (2003).
8. Gregory N., *et al.* Big dung beetles dig deeper: traitbased consequences for faecal parasite transmission. *J. International Journal for Parasitology.* **45**, 101–105 (2015).
9. Hanks L. M. Influence of the larval host plant on reproductive strategies of cerambycid beetles. *J. Annu. Rev. Entomol.* **44**, 483–505 (1999).
10. Jiang Y., *et al.* Molecular identification of sibling species of *Sclerodermus* (Hymenoptera: Bethyridae) that parasitize buprestid and cerambycid beetles by using partial sequences of mitochondrial DNA cytochrome oxidase subunit 1 and 28S ribosomal RNA gene. *J. PLoS ONE*, **10(3)**, 1–15 (2015).
11. Johnson M. P., *et al.* The effects of dispersal mode on the spatial distribution patterns of *Intertidal molluscs*. *J. Journal of Animal Ecology.* **70(4)**, 641–649 (2001).
12. Kundanati L., Chahare N. R., Jaddivada S., Karkisaval A. G., Gundiah N. Cutting mechanics of wood by beetle larval mandibles. *J. Journal of the Mechanical Behavior of Biomedical Materials*, **112**, 104027 (2020).
13. Lyons C. L., Tshibalanganda M., Plessis A. D. Using CT-scanning technology to quantify damage of the stem-boring beetle, *Aphanasium australe*, a biocontrol agent of *Hakea sericea* in South Africa *J. Biocontrol Science and Technology*, **30(1)**, 33–41 (2020).
14. Lyons C. L., Tshibalanganda M., Plessis A. D. Using CT-scanning technology to quantify damage of the stem-boring beetle, *Aphanasium australe*, a biocontrol agent of *Hakea sericea* in South Africa *J. Biocontrol Science and Technology*, **30(1)**, 1–9 (2019).
15. Ma A. K. W., Alghamdi A. A., Tofailli K., Spyrou N. M. X-ray CT in the detection of palm weevils *J. Journal of Radioanalytical & Nuclear Chemistry*, **291(2)**, 353–357 (2012).

16. Ma A., Alghamdi A. A., Tofailli K., Spyrou N. M. X-ray CT in the detection of palm weevils. J. Journal of Radioanalytical & Nuclear Chemistry, **291(2)**, 353–357 (2012).
17. Mamiya Y. Enda N. Transmission of *Bursaphelenchus lignicolus* (Nematode: Aphelenchoididae) by *Monochamus alternatus* (Coleoptera: Cerambycidae). J. Nematol. **18**, 159–162 (1972).
18. Nowak D.J., Pasek J.E., Sequeira R.A., Crane D.E., Mastro V.C. Potential effect of *Anoplophora glabripennis* (Coleoptera: Cerambycidae) on urban trees in the United States. J. Econ. Entomol. **94**, 116–122 (2001).
19. Taylor K. L. The introduction and establishment of insect parasitoids to control *Sirex noctilio* in Australia. J. Entomophaga, **21(4)**, 429–440 (1977).
20. Togashi K., Kasuga H., Yamashita H., Iguchi K. Effect of host tree species on larval body size and pupal-chamber tunnel of *Monochamus alternatus* (Coleoptera: Cerambycidae). J. Appl. Entomol. Zool. **43(2)**, 235–240 (2008).
21. Wang Q. Evidence for a contact female sex pheromone in *Anoplophora chinensis* (Forster) (Coleoptera: Cerambycidae: Lamiinae). J. Coleop Bull **52**, 363–368 (1998).
22. Wang S.F. *Monochamus alternatus*, Forest insects of China (ed. Xiao G.R.) 483–485 (Chinese Forestry Press, 1992).
23. Chai Z. Q., *et al.* Distribution and population dynamics of *Xylotrechus quadripes* Chevrolat on coffee trunk in Puer. J. Southwest China Journal of Agricultural Sciences, **33(11)**, 2519–2523 (2020).
24. Gao S. K., *et al.* Study on the gallery system of *Monochamus alternatus* Hope. J. Forest Research. **35(2)**, 1–6 (2022).
25. Gao S. Q., *et al.* Distribution of *Monochamus alternatus* on the Trunks of *Pinus massoniana* J. Forest Research, **28(5)**, 708–712 (2015).
26. Gao S., *et al.* Overwintering Characteristics and Cold-Hardiness of Biotype of *Dastarcus helophoroides* (Coleoptera: Bothrideridae) on *Monochamus alternatus* (Coleoptera: Cerambycidae). J. Scientia Silvae Sinicae, **52(3)**, 68–74 (2016).
27. Ge Z., Hou X., Li Z., Zhou Y. Application of Computed Tomography (CT) in Nondestructive Testing of Wood. J. China Wood Industry, **30(3)**, 50–53 (2016).
28. Hao D., Zhang Y., Dai H., Wang Y. Oviposition preference of *Monochamus alternatus* Hope (Coleoptera: Cerambycidae) to host plants. J. Acta Entomologica Sinica, **48(3)**, 460–464 (2005).
29. Hu X., Qu T., Zheng H. Control countermeasures of *Bursaphelenchus xylophilus* in China. J. Forest Pest and Disease, **(3)**, 30–32 (1997).
30. Jiang S. Longicorn larva (ed. Jiang S.) 1–8 (Chongqing Press, 1989).
31. Liu Qizhi, *et al.* Biology of RNL's Boring Trunk and Expelling Farass. J. Journal of China Agricultural University, **4(5)**, 87–91 (1999).
32. Liu Y., Zhao H. A preliminary study on the *Apriona swainsoni* larval boring and wormhole system. J. Plant Protection. **35(6)**, 119–122 (2009).

33. Lv F., *et al.* Review of the tritrophic interactions of plant-trunk borer-natural enemy. *J. Forest Pest and Disease*, **34(2)**, 35–39 (2015).
34. Niu Y., *et al.* Study on Frass Extruded by Larvae of *Anoplophora glabripennis*. *J. Forest Research*, **23(1)**, 114–119 (2010).
35. Su M., *et al.* Test of pheromone attractant to trap bark beetle in timber. *J. Plant Quarantine*, **22(2)**, 3 (2008).
36. Sun Y., *et al.* Drilling Vibration Identification Technique of Two Pest Based on Lightweight Neural Networks. *J. Scientia Silvae Sinicae*, **56(3)**, 103–111 (2020).
37. Tang C., *et al.* Biological characteristics of *Monochamus alternatus* 生活习性. *J. Journal of Biosafety*. **14(3)**, 209–213 (2005).
38. Tang Y., *et al.* Distribution Pattern of Larvae and Pupae of *Massicus raddei* in the Trunk of *Quercus liaotungensis*. *J. SCIENTIA SILVAE SINICAE*, **47(3)**, 117–123 (2011).
39. Wang Q., *et al.* Application of 3D printing technology in clinical medicine. *J. Medical & Pharmaceutical Journal of Chinese People's Liberation Army*, **31(8)**, 112–116 (2019).
40. Wang X., Yang Z. Zhang Y., Tang Y. Distribution of *Apriona swainsoni* larva on the trunk of *Sophora japonica* and the establishment of its population prediction model. *J. Forest Pest and Disease*, **34(1)**, 20–22 (2015).
41. Wang Y., Luo Y., Zhang Y., Ren L. Adaptability of external morphological structures and capacity for crop damage of some cerambycid larvae. *J. Chinese Journal of Applied Entomology*, **50(3)**, 790–799 (2013).
42. Wei J., Yang Z., Dai J., Du J. Tritrophic system of tree-trunkborer-insect natural enemy association. *J. Chinese Journal Of Applied Ecology*, **18(5)**, 1125–1131 (2007).
43. Wen X., *et al.* The spatial structure and distribution pattern of *Monochamus alternatus* Hope larvae on the bait-trees in *Pinus massoniana* forests. *J. Journal of Southern Agriculture*, **49(10)**, 1995–2000 (2018).
44. Yang B., *et al.* The Latent Infection of *Bursaphelenchus xylophilus* and A New Transmission Way of PWN by *Monochamus alternatus*. *J. Forest Research*, **15(3)**, 251–255 (2002).
45. Yang H., *et al.* A Study on the Spatial Distribution Pattern and the Living-inhabiting Tunnel of the Larvae of *Batocera horsfieldi* (Hope). *J. Journal of Sichuan Agricultural University*, **28(2)**, 148–152 (2010).
46. Zhang Y., *et al.* Biocontrol of the Overwinter *Monochamus alternatus* with *Dastarcus helophoroides*. *J. Scientia Silvae Sinicae*, **50(3)**, 92–98 (2014).
47. Zhao J. The Study of Living and Inhabiting Tunnel of *Monochamus alternatus*. *J. Forest Research*, **18(1)**, 62–65 (2005).

## Figures

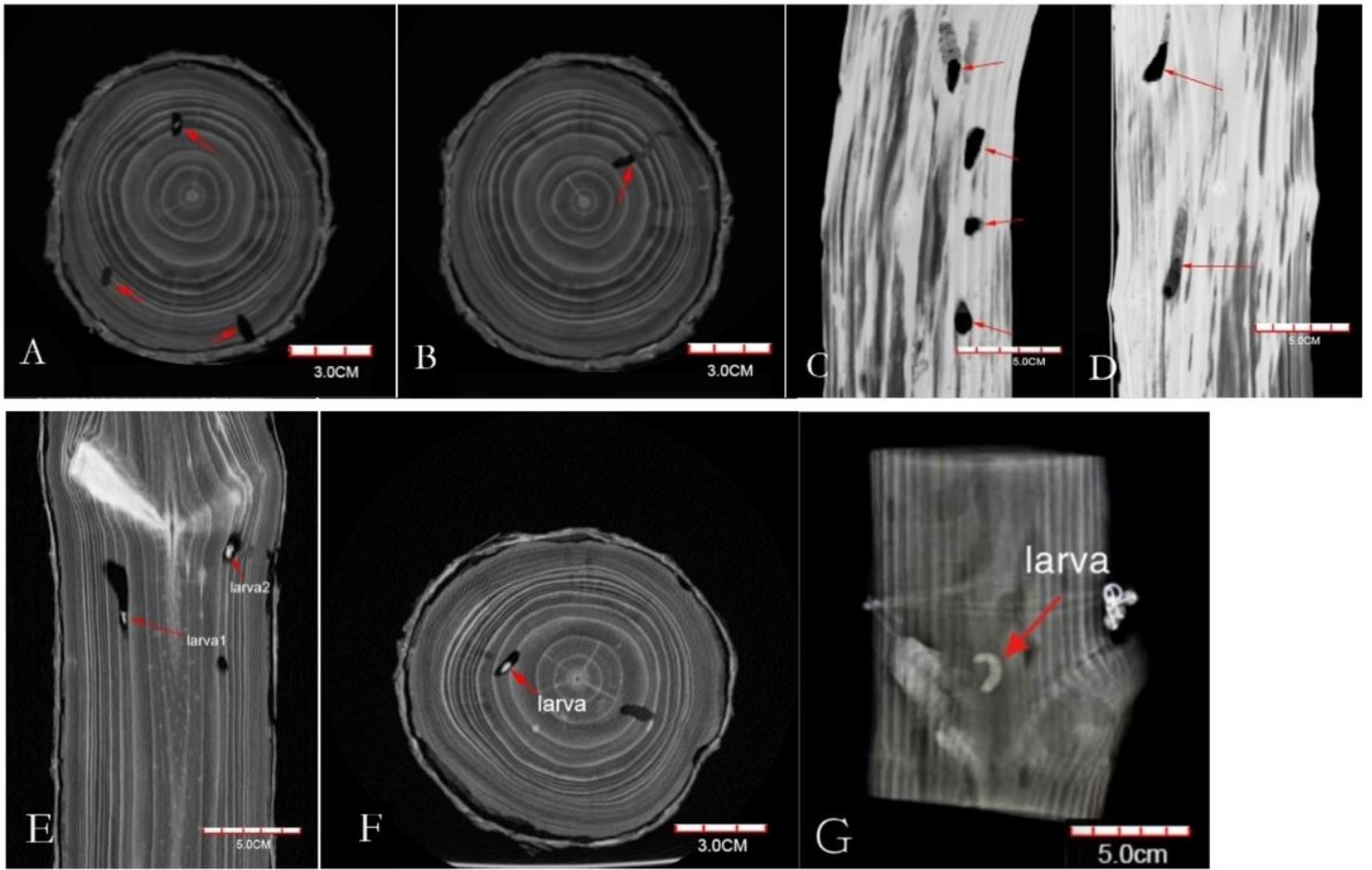


**Figure 1**

CT scanning images of *Pinus densiflora* segments (A and B are on the transverse plane, C and D are on the longitudinal plane, and E, F and G are *Monochamus alternatus* larvae).

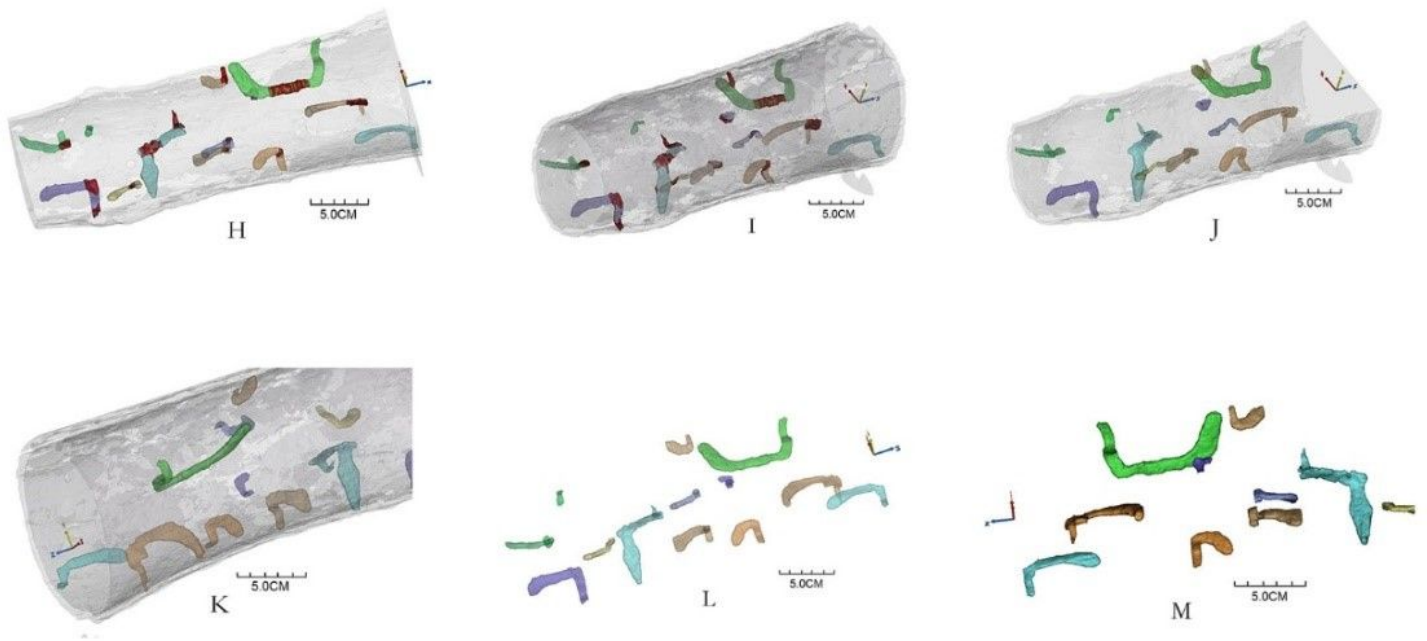


**Figure 2**

Three-dimensional reconstruction of *Monochamus alternatus* gallery structures.

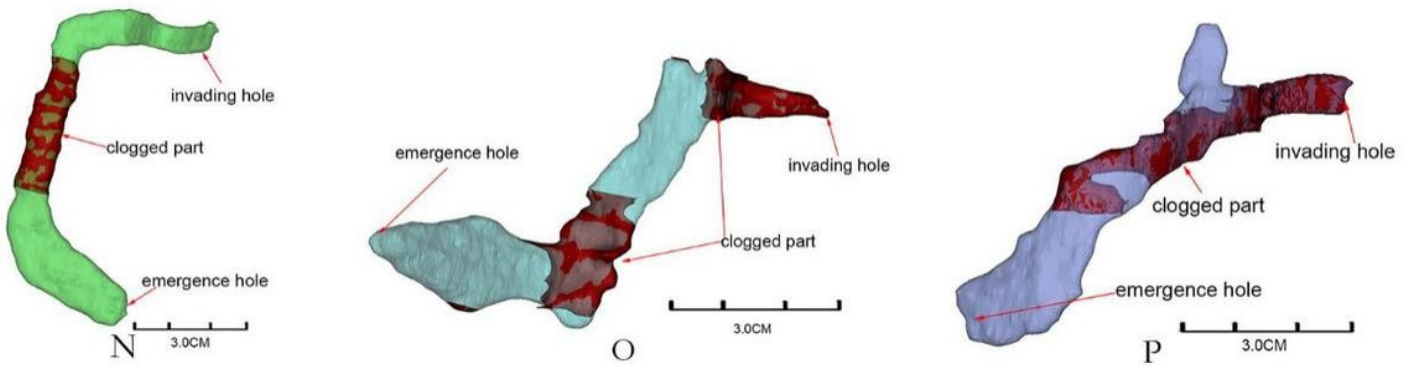


**Figure 3**

Gallery types of *Monochamus alternatus* (N: C-shaped, O: S-shaped, P: Y-shaped).

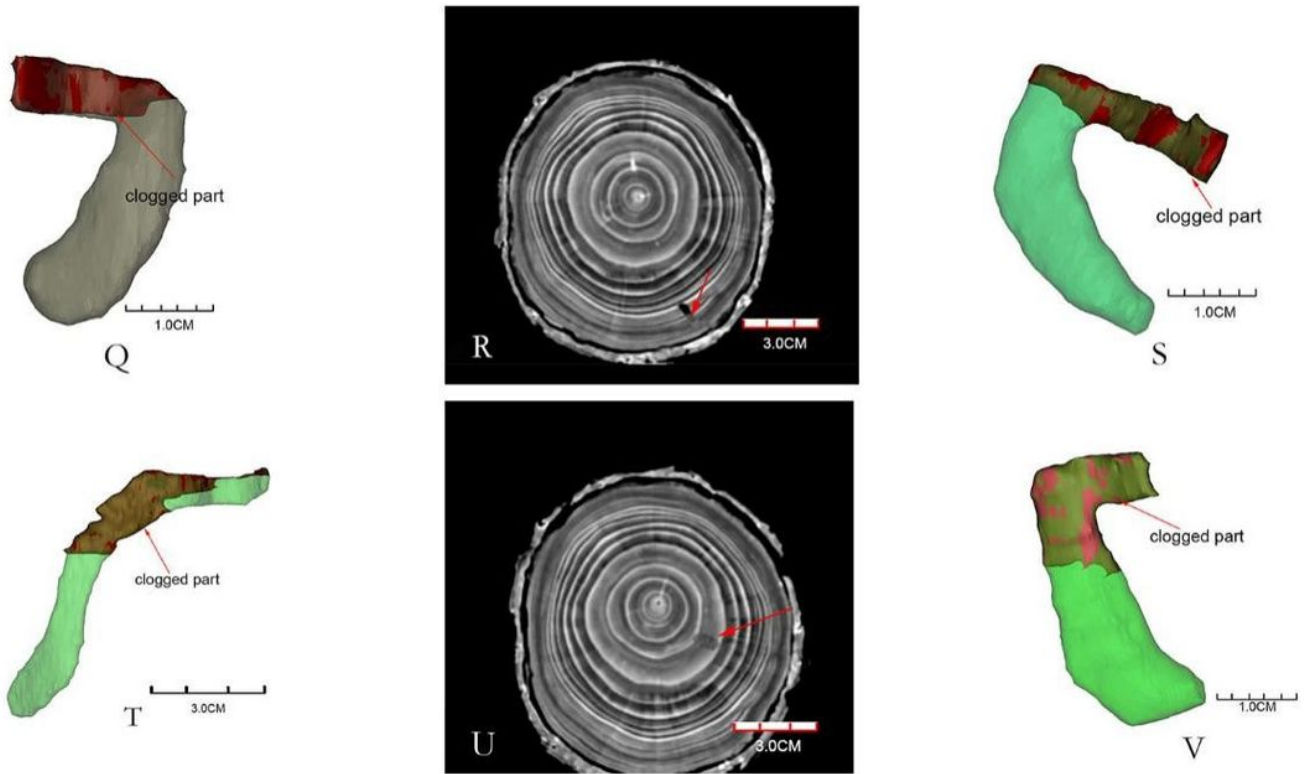


**Figure 4**

Blocked parts of *Monochamus alternatus* galleries. (Q, S, V: the blocked parts of C-shaped are at the beginning of the galleries; T: the blocked part of S-shaped is located in the middle of the gallery. R, U: the images of the transverse section of the CT images of the galleries, note the degree of blockage of the galleries by frass-feces mixture (red arrow))